Mass-Transport Dynamics, Activity, and Structure of Sulfate-Reducing Biofilms

Haluk Beyenal
Center for Biofilm Engineering, Montana State University, Bozeman, MT 59717

Zbigniew Lewandowski
Center for Biofilm Engineering and Dept. of Civil Engineering, Montana State University, Bozeman, MT 59717

Factors limiting hydrogen sulfide production were identified in a two-species biofilm containing sulfate-reducing bacteria (Desulfovibrio desulfuricans) and nonsulfate-reducing bacteria (Pseudomonas fluorescens). Profiles of hydrogen sulfide (H_2S) concentration, pH, local mass-transport coefficient, local flow velocity, and local relative effective diffusivity in the biofilm were measured using microelectrodes. Biofilms had a heterogeneous structure consisting of cell clusters separated by voids. Typically, the H_2S concentration was lower in the voids than in the adjacent cell clusters, demonstrating that the voids acted as transport channels for removing H_2S from cell clusters. The extent of biofilm heterogeneity was directly correlated with the flux of H_2S from cell clusters. At flow velocities below 2 cm/s, the flux of H_2S from cell clusters depended on the flow velocity. We concluded that at these flow velocities the H_2S production rate was limited by the delivery rate of sulfate ions to the biofilm. At flow velocities above 2 cm/s, the H_2S production rate was nearly constant and did not depend on the flow velocity. At high flow velocities (> 2 cm/s) the H_2S production rate was limited by metabolic reactions in the biofilm. Local intrabiofilm flow velocity profiles were influenced strongly by biofilm heterogeneity without significant pH variation within biofilms. Surprisingly, profiles of local relative effective diffusivity indicated that the biofilm was made up of two layers, which could be related to the specimen with a two-species biofilm.

Introduction

Hydrogen sulfide (H_2S) produced by sulfate-reducing bacteria (SRB) can be used to precipitate contaminant metals in water as metal sulfides. For example, Castro et al. (1999) used SRBs to remove arsenic and iron from a pit lake; Shokes and Möller (1999) and Elliot et al. (1998) used SRBs to remove metals from an acid mine drainage; Lloyd et al. (1998) used them to precipitate technetium; and Coleman et al. (1993) used them to reduce ferric iron [Fe (III)] to ferrous iron [Fe(II)].

There is considerable interest in using biofilms containing SRB to immobilize metals in subsurface environments (Lovley and Phillips, 1992, 1994; Coleman et al., 1993; Bidoglio et al., 1993). To optimize the performance of such systems it is important to maximize the production of H_2S. The rate of H_2S production in biofilms containing SRBs may be limited by the availability of sulfate (limited by mass transport) or limited by the SRBs' metabolic activity in the biofilm (limited by the reaction rate). To find out which process limits H_2S production in a specific case, it is useful to quantify both mass-transport dynamics and SRB activity in the biofilms. Biofilm activity can be evaluated at the macroscale, using mass balances around the reactor, or at the microscale, from fluxes of H_2S calculated from concentration profiles measured by microelectrodes (Kühl et al., 1998; Kühl and Jörgensen, 1992). Mass-transfer dynamics can be quantified at the microscale using local mass transport, local flow velocity, and local effective diffusivity microelectrodes (Yang and Lewandowski, 1995; Xia et al., 1998; Beyenal and Lewandowski, 2000).

Correspondence concerning this article should be addressed to Z. Lewandowski.

The goal of this study was to identify factors limiting H_2S production in mixed culture biofilms, consisting of an SRB, *Desulfovibrio desulfuricans*, and a non-SRB, *Pseudomonas fluorescens*, grown in flat-plate reactors. Using microscope images we quantified the structural heterogeneity of the biofilms. The H_2S concentration, local mass-transfer coefficient, local flow velocity, local effective diffusivity, and pH profiles were measured using microelectrodes. The major factor influencing mass-transport rates in biofilms is hydrodynamics. By varying the bulk flow velocity during measurements, we quantified the influence of mass transport on H_2S production.

Experimental Methods

Organisms

We used mixed culture biofilms of *D. desulfuricans* (G20) and *P. fluorescens* (ATCC 700830). The *D. desulfuricans* (G20) were developed from G100A donated by J. D. Wall (Wall et al., 1993), and the *P. fluorescens* (ATCC 700830) was an environmental isolate from our laboratories. A fresh inoculum for each experiment was prepared by growing a one-day-old batch culture of *P. fluorescens* and a 3-day-old batch culture of *D. desulfuricans*. The reactors were inoculated with 20 mL of each culture.

Nutrient solution

We used Postgate medium C without $FeSO_4$, including sodium lactate (Sigma) (Postgate, 1984); we removed $FeSO_4$ from the solution to prevent FeS precipitation in the biofilm. The pH of the solution was adjusted to 7.2 using NaOH. Resuzirin (0.5 mg/L) was added to the growth medium to test for anaerobic conditions.

Experimental setup and procedure

The biofilms were grown at room temperature on microscope slides (2.5×7.5 cm) placed on the bottom of an open-channel flow reactor made of polycarbonate (3.5 cm deep, 2.5 cm wide, and 34 cm long, with a total working volume of 120 mL). A view of the experimental setup is presented in Figures 1A and 1B. The lid of the reactor was sealed with silicon rubber to prevent contamination, and the entire system was sterilized with 70% alcohol before each experiment. The reactor was then rinsed with sterile water (autoclaved) until all the alcohol was removed. Tubings, connectors, air filters and the growth medium were also autoclaved at 121°C. Before the addition of the growth medium and during biofilm growth, the system was continuously purged with nitrogen gas to create positive pressure and prevent oxygen penetration into the system.

For microelectrode measurements, the microscope slides from the growth reactor were transferred to another reactor, positioned on an inverted microscope, and operated at the same experimental conditions. Microscopic examinations, before and after the slide was moved to the other reactor, showed that the biofilm structure remained the same. The microscope slides holding the biofilm were allowed to re-equilibrate in the nutrient solution for 6 h before microelectrode measurements were taken. For the measurements at different flow velocities, we waited for 2–3 h to give the biofilm time to adapt to each new flow velocity. Anaerobic conditions were tested in each case.

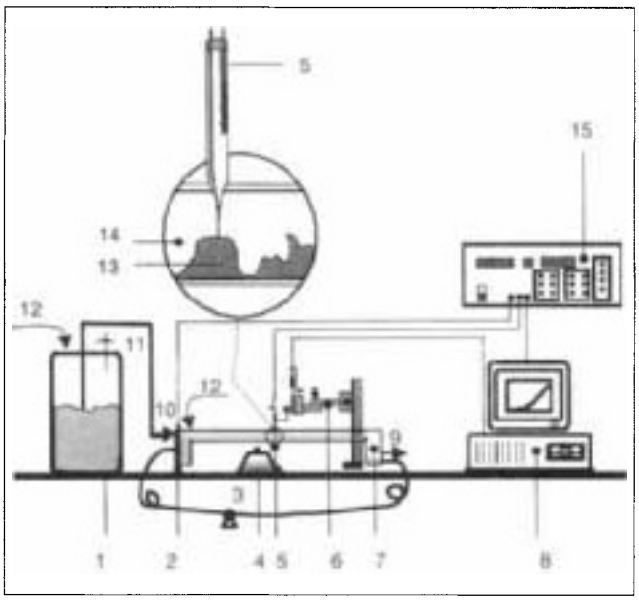

Figure 1a. Experimental setup.

(1) Growth medium; (2) reference electrode*; (3) peristaltic pump; (4) inverted microscope; (5) microelectrode*; (6) micromanipulator*; (7) flat-plate flow cell; (8) computer*; (9) outlet; (10) fresh feed; (11) vent; (12) nitrogen gas; (13) cell cluster; (14) interstitial void; (15) picoammeter.* (*) These instruments were used only during measurements.

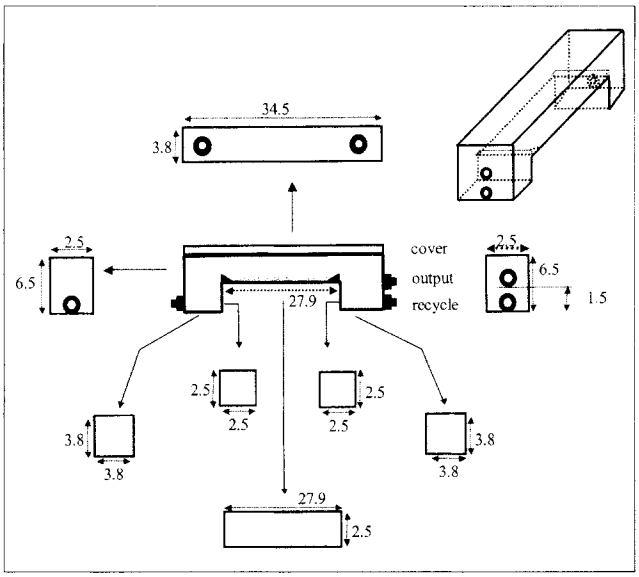

Figure 1b. Flat-plate flow cell constructed of polycarbonate (1/4-in., 6.4-mm, thick).

All fittings are 3/8-in. (9.5-mm) opening width with 1/8-in. (3.2-mm) plastic pipe thread (ACE Hardware Corp., Oak Brook, IL). All fittings are centered and placed close to the edge except the output line, which is positioned above the recycle line. All dimensions are in cm and the figure is sketched without scale.

Sodium sulfate and magnesium sulfate were used as a source of sulfate, and the concentration of sulfate ions was measured by the barium-sulfate turbodimetric method (APHA 1995). Based on these measurements, the sulfate loading rate was calculated as mM sulfate fed to the reactor per unit of time. We calculated the load per unit of time because the actual biofilm surface area was unknown in the reactor. Before each analysis liquid samples were filtered using 0.2 μm Nuclepore filters.

Microelectrodes and measurement techniques

We used three types of microelectrodes in this study: H_2S, pH, and limiting current microelectrodes for measuring mass-transport coefficient, local effective diffusivity, and local flow velocity. The microelectrodes had tip diameters less than 10 μm to prevent damaging the biofilm structure during measurements.

H_2S Microelectrode. We constructed H_2S microelectrodes according to Jeroschewski et al. (1996). The construction was similar to that of Clark-type dissolved-oxygen microelectrodes. The H_2S diffuses through the silicone membrane at the tip to the shaft of the microelectrode, which is filled with an alkaline solution of potassium ferricyanide ($K_3Fe(CN)_6$). In this solution, part of the H_2S was deprotonated to HS^-, which was then oxidized to S^0 by the ferricyanide. The reduced form of ferricyanide, ferrocyanide ($K_4Fe(CN)_6$), was then reoxidized to ferricyanide at the internal platinum anode polarized to (+)100 mV against a counterelectrode placed 10 μm behind the silicone membrane. The electrode was calibrated in solutions of different H_2S concentration; and the current generated by oxidizing ferro- to ferricyanide was proportional to the H_2S concentration near the tip of the microelectrode. The response time of the microelectrodes was less than 0.3 s and was linear over a large concentration range, from 0 to 2000 μM H_2S. The microelectrodes had the same calibration before and after the measurements, within the range of acceptable experimental error.

pH Microelectrode. The pH microelectrodes were constructed according to Thomas (1978), using pH-sensitive glass (Corning 0150) for the tip of the microelectrode. We could not use liquid-ion exchanger-tip membranes because of possible interactions between the membrane material and the microbially generated H_2S. Glass-membrane pH microelectrodes had stable and reproducible calibration curves with a typical slope of 58 mV/pH.

Limiting-Current-Type Microelectrodes to Measure Local Mass-Transfer Coefficient, Local Effective Diffusivity, and Local Flow Velocity. Limiting-current microelectrodes were constructed with tip diameters less than 10 μm, using an electrochemically tapered platinum wire, without membrane. All microelectrodes used in this project were previously constructed, tested in our laboratory, and described elsewhere. The construction of the local mass-transfer coefficient microelectrodes was described by Yang and Lewandowski (1995); local effective-diffusivity microelectrodes by Beyenal and Lewandowski (2000); and local flow-velocity microelectrodes by Xia et al. (1998). Here we provide only a brief description of the technique.

Limiting-current-type sensors belong to a large group of amperometric sensors in which their principal use is measuring the current generated by reducing (or oxidizing) electroactive materials at surfaces of electrically polarized electrodes [see Mizushina (1971) and Selman and Tobias (1978) for details]. The current measured by these devices is equivalent to the rate of the electrode reaction, which is determined by the applied potential and the rate at which the reactant arrives at the electrode (mass-transport rate).

To apply the limiting-current-type microelectrodes to measure mass-transport coefficients in biofilm systems, two conditions need to be satisfied: (1) the only sink for the electroactive substance in the system must be the microelectrode tip, and (2) there can be only one electroactive substance available for the electrode to process at a time. We use mobile microelectrodes and expose their tips at various locations in biofilms. As the electroactive reactant we use a 25-mM solution of potassium ferricyanide, $K_3Fe(CN)_6$, in 0.2 M KCl. With proper experimental control, the ferricyanide is reduced to ferrocyanide, $Fe(CN)_6^{4-}$, at the surface of cathodically polarized microelectrodes. At limiting current, the concentration of ferricyanide at the electrode surface is zero ($C_s = 0$), while in the bulk solution it remains (C_o). The concentration gradient is said to be confined entirely within the mass-transfer boundary layer. For these assumptions the mass-transfer coefficient is related to the measurable parameters and constants by the following equation

$$k = I/nAFC_o. \tag{1}$$

Here F is Faraday's constant, n is the number of electrons transferred in the balanced reaction, A is the sensing area of the electrode, and I is the limiting current.

Microelectrode measurements

The microelectrodes were inserted into the reactor through a small opening in the lid while nitrogen gas continuously purged the system, creating a positive pressure in the reactor and preventing ingress of air from the outside. The microelectrodes were mounted on a micromanipulator (Model M3301L, World Precision Instruments, New Haven, CT) equipped with a stepper motor (Model 18503, Oriel, Stratford, CT) controlled by the Oriel Model 20010 interface. Microelectrodes were introduced from the top of the reactor at an angle perpendicular to the biofilm. The micropositioner was interfaced with a computer, and the microelectrode movement was handled by a controller (CTC-283-3, Micro Kinetics) with a positioning precision of 0.1 μm. Custom software was used to control and coordinate microelectrode movement and data acquisition. Details of the measurement procedure have been described by Beyenal and Lewandowski (2000). The diffusive fluxes of H_2S to the bulk liquid were calculated by multiplying the slope of the profiles evaluated at the biofilm surface by the diffusion coefficient of H_2S in water ($D_{H_2S} = 1.7 \times 10^{-5}$ cm^2/s) (Kühl et al., 1998).

For limiting-current-type microelectrode applications—mass transfer, flow velocity, and effective diffusivity—the reactor was opened to the atmosphere because these measurement systems did not require anaerobic conditions. Technically, the microelectrodes to measure local mass-transfer coefficient, local flow velocity, and local effective diffusiv-

ity all worked on the same principle: a cathodically polarized microelectrode measures the limiting current at different locations in a biofilm. The differences in experimental conditions and microelectrode calibration procedures define what is actually measured. The local mass-transport coefficients and local flow velocities are measured in solutions of flowing electrolytes because the convective mass-transport component must be included in the final result. To measure the local effective diffusivity we use the same system, but the flow is stopped and the measured limiting current reflects only the diffusional component of the mass transport.

Before taking the measurements, the growth medium in the reactor was replaced with 25 mM $K_3Fe(CN)_6$ in 0.2 M KCl. This electrolyte solution was recycled for 2 h before the measurements to equilibrate the biofilm with the ferricyanide. The system was flushed with enough ferricyanide to remove all H_2S and other reactive chemicals from the biofilm. We previously demonstrated that this procedure did not change the biofilm structure (Beyenal and Lewandowski, 2000; Yang and Lewandowski, 1995).

Microscopy, biofilm imaging, and structure quantification

The flat-plate reactor was placed on the Nikon Diaphot 300 inverted microscope, and the biofilm was viewed using UV light projected through the bottom. Images were captured by a COHU camera (Closed Circuit, CA, model No. 2222-1040/0000) and a Flashpoint frame grabber (Integral Technologies Inc., Indianapolis, IN) connected to a computer. The images were taken in 8-bit gray-scale TIFF format, consisting of 640×480 pixels using Image Pro custom software (Media Cybernetics, MD). From the biofilm images we determined the values of areal porosity, fractal dimension, and total length of cell cluster perimeters. The structure parameters were calculated using the Image Structure Analyzer (ISA), a software package developed for the purpose of quantifying biofilm structure (Yang et al., 2000). This imaging system was also used to move the microelectrode to the same position for different type of measurements.

Results and Discussion

Biofilm structure

A gray-scale image of a 5-week-old mixed-culture biofilm is shown in Figure 2 along with measurement points. This biofilm structure was heterogeneous, consisting of voids and cell clusters. For the measurements we selected five locations in voids and in clusters. Measurement point 1 is a big, open void (around 80 μm wide) parallel to the flow direction. Point 2 is located very close to the end of the channel (100 μm in diameter), which is also parallel to flow direction. Point 3 is in the middle of a small closed void (40 μm in diameter). Point 4 is the center of a big cluster (250 μm in diameter), and point 5 is the edge of the cell cluster and very close to point 1. The average biofilm thickness was around 800 μm, areal porosity was 0.34, and fractal dimension was 1.1952.

The mixed-culture biofilms of *D. desulfuricans* and *P. fluorescens* developed a heterogeneous structure, similar to that observed by Power et al. (1999) and Santegoeds et al. (1998). A sample image marked at points where profiles were measured is presented in Figure 2. We also took images at other

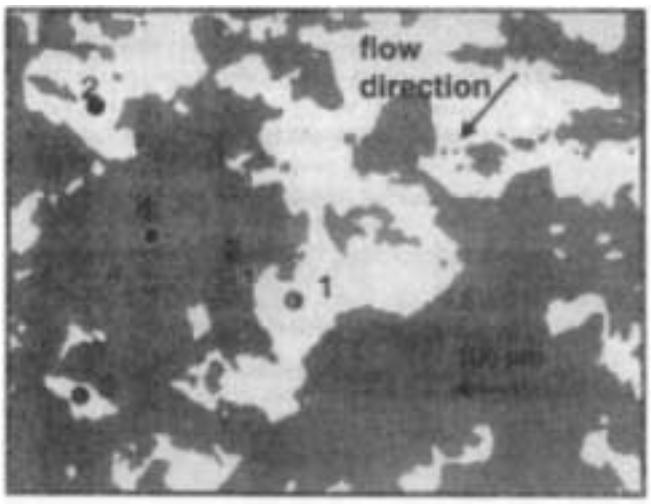

Figure 2. Five-week-old biofilm consisting of *D. desulfuricans* and *P. fluorescens*.

Light areas are voids and dark areas are cell clusters. The numbers indicate locations of the measurements: (1) big void; (2) midsize void; (3) small void; (4) cluster center; (5) cluster edge. The biofilm was grown at a flow velocity of 2 cm/s using Postage C growth medium under anaerobic conditions.

locations in the biofilms, and they all looked similar to that in Figure 2. The values of the structure parameters (areal porosity and fractal dimension) oscillated within $\pm 5\%$ of the average value. The areal porosity and fractal dimension showed lower heterogeneity of this biofilm compared to aerobic biofilms (Lewandowski et al., 1999; Gibbs and Bishop, 1995). Possible extension of this study to biofilms with varying heterogeneity may help future biofilm modeling, as described at the end of this article.

H_2S concentration profiles and fluxes

H_2S profiles measured at selected locations are presented in Figures 3 and 4 at two flow velocities: 0.8 cm/s and 2 cm/s. The H_2S fluxes calculated from these profiles are shown in Table 1.

For a flow velocity of 0.8 cm/s, the H_2S concentration in the bulk solution was found to be around 80 μM. The H_2S concentrations near the bottom of the voids were 120, 115, and 85 μM for small, medium, and big voids, respectively (Figure 3A). For a flow velocity of 2 cm/s, the H_2S concentration in the bulk solution was around 86 μM. The H_2S concentrations near the bottom of the voids were 137, 122 and 96 μM for small, medium, and big voids, respectively (Figure 3B).

For a flow velocity of 0.8 cm/s, the H_2S concentrations near the bottom at the center of the cell cluster (point 4 in Figure 2), and at the edge of the cell cluster (point 5 in Figure 2), were 170 and 153 μM, respectively. For a flow velocity of 2 cm/s, the H_2S concentrations measured near the bottom and at the center of the cell cluster (point 4 in Figure 2), and at the edge of the cluster (point 5 in Figure 2), were 174 and 159 μM, respectively.

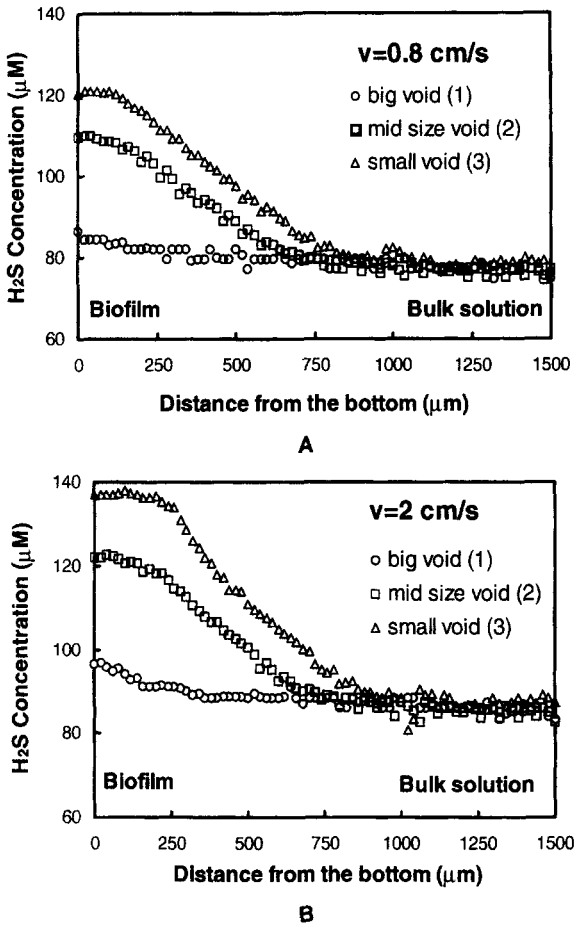

Figure 3. H_2S concentration profiles measured in voids at the bulk flow velocity (A) 0.8 cm/s and (B) 2 cm/s.

The diffusive fluxes were determined by multiplying the slopes of the profiles measured at the approximate position of the surfaces of the adjacent microcolonies, between 500 and 700 μm, by the molecular diffusivity of H_2S in water. Although the average biofilm thickness was 800 μm, this thickness was decreasing near the voids, because of the heterogeneous structure of the biofilm.

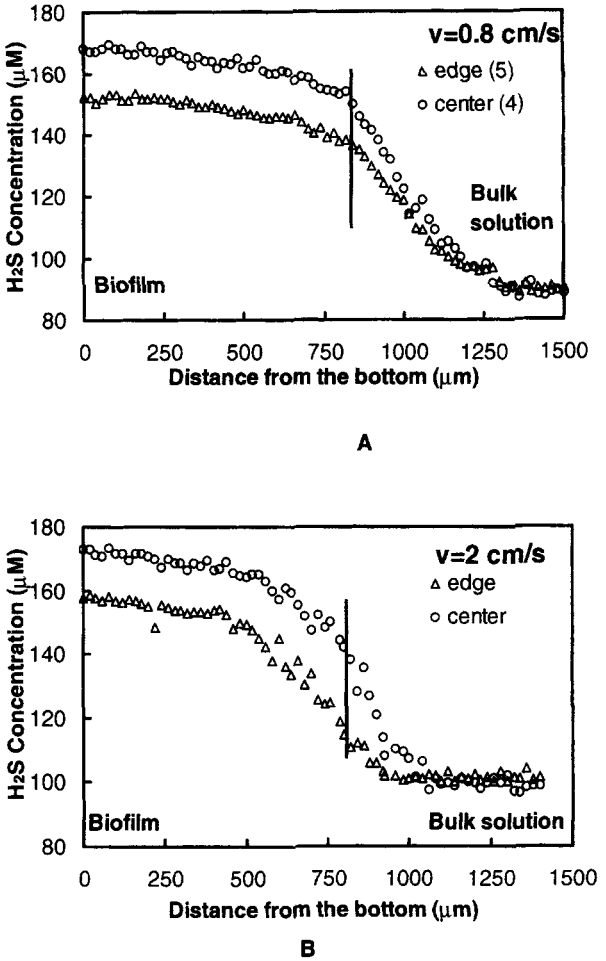

Figure 4. H_2S concentration profiles measured at the edge and center of the cell cluster presented in Figure 2 at a bulk flow velocity of (A) 0.8 cm/s and (B) 2 cm/s; the continuous line shows the location of the biofilm surface.

The increasing bulk flow velocity, from 0.8 cm/s to 2 cm/s, increased the H_2S flux from the voids (see Table 1), and these effects were more noticeable with increased void size. The percentage increase of the fluxes for the increasing flow velocity from 0.8 cm/s to 2 cm/s for the voids 1, 2, and 3 were 23, 16, and 7, respectively. The H_2S concentrations were lower in voids than in adjacent cell clusters, showing that voids acted as transport channels for removing H_2S from the cell clusters (Figures 3 and 4).

Fluxes of H_2S out of the cell clusters were strongly affected by the bulk flow velocity. For example, when the flow velocity increased from 0.8 cm/s to 2 cm/s, the H_2S fluxes out of the cell clusters increased by 47% (from 2.28×10^{-6} μmoles/cm^2/s to 2.70×10^{-6} μmoles/cm^2/s) near the cluster edge and by 92% (from 2.22×10^{-6} μmoles/cm^2/s to 4.18×10^{-5} μmoles/cm^2/s) near the cluster center. The increase of the bulk flow velocity increased H_2S concentrations at the center and the edge of the cell cluster (Figure 4); however, the flux of H_2S increased more at the center of the cluster than at the edge.

Sulfate loading and H_2S production rates

Figure 5 shows the variations of the H_2S flux as a result of the sulfate loading rate, measured at the center of the cluster (point 4 in Figure 2), at a bulk flow velocity of 2 cm/s. The H_2S production rate increased to a maximum value of 2.7×

Table 1. H_2S Fluxes Calculated from Local Profiles

Location	H_2S Flux (μmoles/cm^2/s)	
	Bulk Flow Vel. of 0.8 cm/s	Bulk Flow Vel. of 2 cm/s
1. Big void	8.35×10^{-6}	1.1×10^{-5}
2. Midsize void	7.06×10^{-6}	8.45×10^{-6}
3. Small void	7.23×10^{-7}	7.22×10^{-7}
4. Cluster center	2.22×10^{-6}	4.18×10^{-5}
5. Cluster edge	2.28×10^{-6}	2.70×10^{-6}

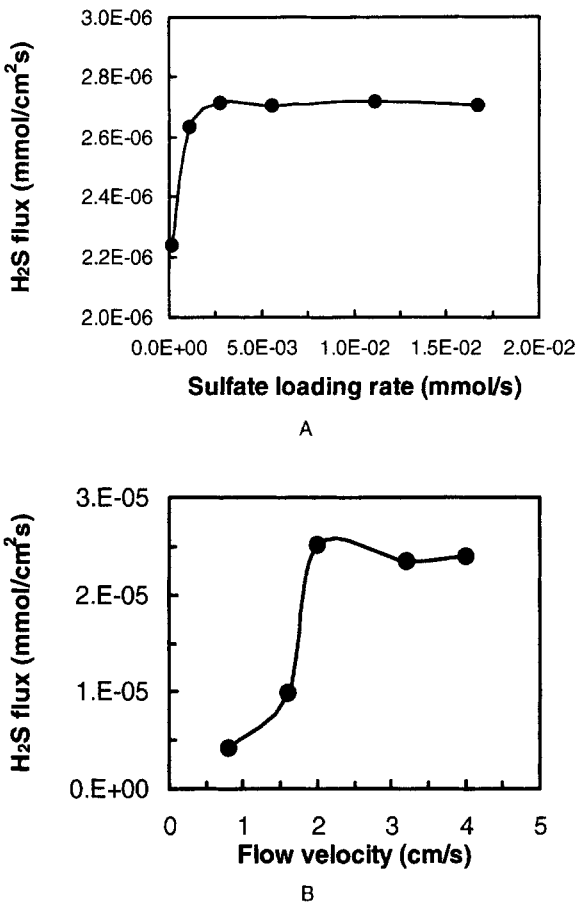

Figure 5. (A) H_2S flux to the bulk water at the center of the cluster (point 4 in Figure 2) at different sulfate loading rates; flow velocity was 2 cm/s; (B) the H_2S fluxes at different flow velocities at 0.02 mmoles/s sulfate loading rate.

10^{-6} μmoles/cm^2/s at 2.5×10^{-3} mmoles/s sulfate loading rate and then remained constant for higher loading rates.

The H_2S fluxes measured at different flow velocities and at a constant, 0.02 mmoles/s sulfate loading rate, are presented in Figure 5B. The H_2S flux reached a maximum of 2.7×10^{-6} μmoles/cm^2/s at 2 cm/s flow velocity. Further increases in bulk flow velocity did not influence the activity of the biofilm. From mass balances, input minus output, for sulfate, SO_4^{2-}, and H_2S, we estimated that 75% of the sulfate was converted to sulfide. The calculated conversion ratio of sulfate to sulfide, 0.75, was lower than the 0.98 observed by Kühl et al. (1998).

Figure 5 shows that at low flow velocities (< 2 cm/s) H_2S production is limited by external mass transfer. Increasing the flow rate above 2 cm/s did not change the H_2S production rate, possibly because the production rate was already at the maximum and was reaction rate limited. Another possible explanation is that the H_2S concentration became inhibitory; however, the H_2S concentrations in our biofilms were at least three times lower than the inhibitory concentration observed by Okabe et al. (1995) for pure culture *D. desulfuricans*, and this explanation is rather unlikely.

The flux of H_2S was not affected by a sulfate loading rate higher than 2.5×10^{-3} mmoles/s (Figure 5A). In our experiments, the sulfate loading rate was higher than 0.02 mM/s, which is eight times higher than the limiting loading rate, and we can safely conclude that sulfate delivery rate was not a limiting factor.

Local mass-transfer coefficient

Microelectrode measurements of H_2S concentrations and experiments at different sulfate loading rates showed that the H_2S concentration and sulfate availability were not limiting H_2S production. The remaining two factors that could limit H_2S production were internal mass-transport rates and activity of the microorganisms. Consequently, we decided to quantify the internal mass-transport dynamics by measuring the local mass-transport coefficient.

Local mass-transfer coefficients measured at the center of the cell cluster (point 4 in Figure 2) at flow velocities of 0.8, 2, 3.2 and 4 cm/s are presented in Figure 6. The local mass-transfer coefficients, normalized with respect to the maximum value measured at a 4-cm/s flow velocity, were high in the bulk liquid and lower in the biofilm, with the lowest values occurring near the bottom of the biofilm (Figure 6). For a flow velocity of 0.8 cm/s the normalized local mass-transfer coefficient near the bottom of the biofilm was 0.32, and for the flow velocity 4 cm/s it was 0.68. The local mass-transfer coefficient was within the range of previously observed values (Yang and Lewandowski, 1995; Stoodley et al., 1997).

For flow velocities lower than 2 cm/s the H_2S flux from the microcolonies dropped significantly, illustrating the existence of external mass-transport limitation (Figure 5b). However, increasing flow velocities above 2 cm/s did not change the H_2S production rate (Figure 5b). The local mass-transport coefficient increased with increasing bulk flow velocity (Figure 6), showing that more substrate diffused into the biofilm. From the combined measurements of H_2S fluxes (Figure 5) and the local mass-transport coefficient (Figure 6), we concluded that H_2S production is limited by the activity of the microorganisms in the biofilm.

Local flow-velocity profiles

The local flow velocity profiles measured in the voids (points 1, 2, and 3 in Figure 2) at two average flow velocities, 0.8 cm/s and 2 cm/s, are presented in Figure 7.

The results in Figure 7 reflect how the biofilm structures affect the local flow-velocity distribution in voids. The profiles of local flow-velocity were different at each location, demonstrating how the flow-velocity profiles in biofilms are affected by the orientation of voids with respect to the direction of flow. The profiles in Figure 7 show that the highest flow velocity was at point 1 (big void). This observation may be a result of point 1 being located in a channel, which was parallel to the flow direction. The flow velocity at point 2 (midsize void) was lower than that at point 1 because it was close to the end of the channel. The flow velocity at point 3 was lowest in comparison to the other two points because it was a closed channel. Local flow-velocity profiles within the biofilm at each of the three locations marked in Figure 2 are different; however, they all converge to the bulk flow velocities (0.8 cm/s, Figure 7A or 2 cm/s, Figure 7B) at different rates.

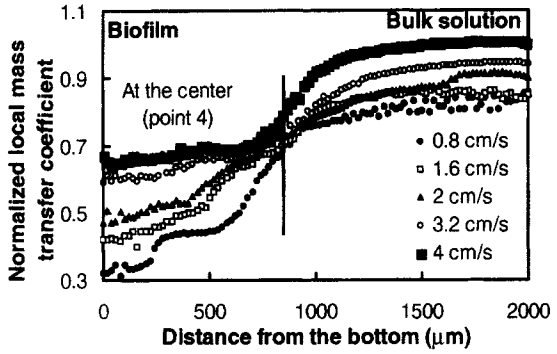

Figure 6. Normalized local mass-transfer coefficient profiles measured at flow velocities of 0.8, 1.6, 2, 3.2 and 4 cm/s.

Increasing the bulk flow velocity increased the local mass-transfer coefficient in the biofilm, showing that more substrate diffused into the biofilm. The continuous line shows the location of the biofilm surface.

Local relative effective diffusivity profiles

An example of a profile of local relative effective diffusivity measured at the center of the cluster (point 5 in Figure 2) is presented in Figure 8. Similar profiles were measured at different locations in the biofilm. We also repeated these measurements in different experiments and consistently observed profiles similar to that in Figure 8. Effective diffusivity seemed to level off at two levels within the biofilm: once just above the bottom and again halfway between the bottom and the surface. The local relative effective diffusivities were consistently around 0.6 near the surface and 0.45 near the bottom.

Consistently, two layers of effective diffusivity were observed during repeated experiments of the SRB biofilms up to 9 weeks old. Fan et al. (1990) showed that biofilm density correlated exponentially with effective diffusivity. Because the major factor influencing effective diffusivity is biofilm density, these two layers of effective diffusivity can be considered as two layers of biofilm density, showing two layers of growth in SRB biofilms, as observed by Power et al. (1999). Similarly, Beech et al. (1991) studied the growth of these microorganisms on metal surfaces and demonstrated that the size of *D. desulfuricans* (2–3 μm) is smaller than that of *P. fluorescens* (3–5 μm). If we assume that smaller microorganisms produce denser biofilms, our results should show *D. desulfuricans* located near the bottom of the biofilm. In a separate experiment, we grew pure-culture biofilms of *D. desulfuricans* at the same conditions and measured diffusivity profiles. The local relative effective diffusivities varied between 0.35 and 0.55, which is consistent with the previous conclusion and indicates the possibility that SRB are located near the bottom in the mixed-culture biofilm. However, further investigations, possibly using fluorescent *in situ* hybridization (FISH probes), are necessary to investigate exact locations of SRB in mixed-culture biofilms (Okabe et al. 1999).

pH profiles

pH profiles, measured at locations specified in Figure 2, did not show any significant pH variation in the biofilms. Fig-

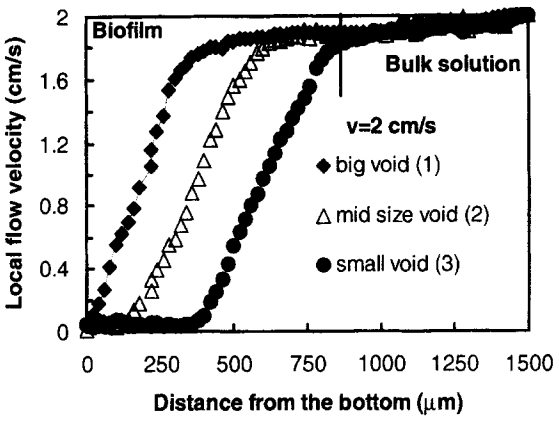

A

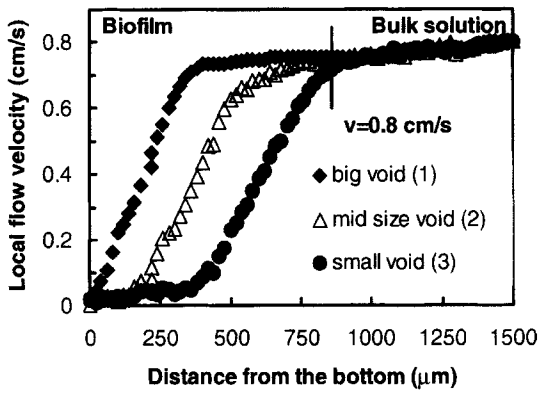

B

Figure 7. Local flow-velocity profiles measured in voids and at two average flow velocities: (A) 0.8 cm/s, and (B) 2 cm/s.

Increased bulk flow velocity increased local flow velocities in voids showing more convectional mass transport in biofilms. Although the average biofilm thickness was 800 μm, this thickness was decreasing near the voids, because of the heterogeneous structure of the biofilm. The continuous line shows the location of the biofilm surface.

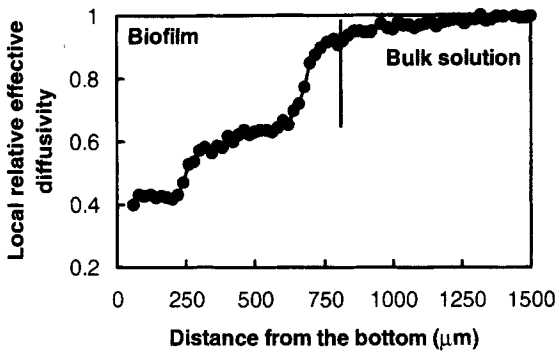

Figure 8. Variation of local relative effective diffusivity with respect to depth in the biofilm.

The continuous line shows the location of the biofilm surface.

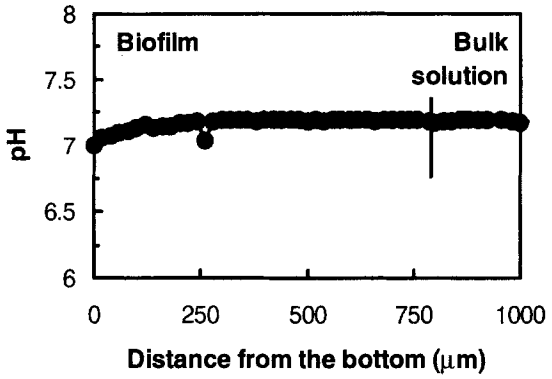

Figure 9. pH as a function of distance from the bottom, measured at the center of the cluster (point 4 in Figure 2).

We measured similar pH profiles at other locations in the biofilm. The continuous line shows the location of the biofilm surface.

ure 9 shows an example of a pH profile measured at the center of the cluster (point 4 in Figure 2). The pH dropped slightly near the bottom. Similarly, insignificant pH variations in biofilms have been observed in SRB biofilms by Okabe et al. (1999 and 1998) and Lee et al. (1994). We measured pH profiles to be sure that these values did not change significantly in the biofilms. The variation in pH influences the ratio of sulfide species present in the biofilm.

Biofilm structure and function

The biofilm in Figure 2 was grown at an average bulk flow velocity of 2 cm/s. We kept the growth conditions constant, and after a steady state was reached, we set the bulk flow velocity at values higher or lower than the 2 cm/s flow velocity at which the biofilm was grown.

When the biofilms were exposed to flow velocities lower than 2 cm/s, the H_2S production dropped significantly. However, when the biofilms were exposed to flow velocities higher than 2 cm/s, the H_2S flux did not depend on flow velocity. We concluded that (1) for flow velocities lower than 2 cm/s, the H_2S production was controlled by mass transport of sulfate to microcolonies, and (2) for flow velocities higher than 2 cm/s, the H_2S production was limited by reaction rate. It is quite interesting to notice that the flow velocity that determined how H_2S production was controlled was exactly equal to the flow velocity at which the biofilm was grown, 2 cm/s.

Hypothetically this result shows that biofilms arrange their structure during their growth to minimize external mass-transfer limitations by adjusting pore structure or surface roughness. We know that the increased surface roughness or increased pore size increases the mass-transport rate to the biofilm (Smets et al., 1999; Tanyolaç and Beyenal, 1997; Peyton, 1996; Murga et al., 1995). It is possible that biofilms adjust the extent of heterogeneity during their growth to minimize external mass-transport limitations and to maximize internal substrate consumption rates.

Biofilm structure, mass transport, and modeling

Picioreanu et al. (2000) modeled mass transport in heterogeneous biofilms. Our experimental results did not verify these model predictions. For example, the model predicts that a 4-fold increase of mass-transfer coefficient requires a 128-fold increase in bulk flow velocity. According to our experimental observations, the local mass-transfer coefficient doubled with a 5-fold increase in bulk flow velocity (Figure 6), a value that was much lower than expected based on the model. Also, the shape of local flow velocity profiles (Figure 7) and model predictions are different. This difference can be caused by the fact that the model assumes insignificant convective transport in voids. In this, and in our previous study (Xia et al., 1998), we showed significant convective mass transport in voids (see Figures 3 and 7); however, we believe that the main reason for the differences between the experimental observation and the model predictions are related to the fact that it was a 2-D (not a 3-D) model. The authors mentioned the necessity of 3-D biofilm modeling for realistic predictions. Our data can be used to verify such a 3-D biofilm model once one is constructed.

Conclusions

1. The mixed culture of *D. desulfuricans* and *P. fluorescens* biofilms had a heterogeneous structure consisting of voids and cell clusters.

2. H_2S concentration varied among locations in the biofilm (higher in the cell clusters and lower in the voids), showing that the voids acted as transport channels to deliver sulfate to the cell clusters and remove H_2S from them.

3. For flow velocities less than 2 cm/s, the H_2S production rate was limited by the rate of external mass transfer, and for flow velocities higher than 2 cm/s, the H_2S production rate was limited by microbial activity. Coincidentally, 2 cm/s was the flow velocity at which the biofilms were grown, and it was the optimum flow velocity at which mass-transfer rate and microbial reaction rate were balanced. Based on this, it can be speculated that the biofilm adjusted its structure to maximize the transport of nutrients to the microcolonies.

4. The extent of biofilm heterogeneity strongly influenced the local flow velocity profiles and rates of the intrabiofilm mass transport.

5. Surface-averaged relative effective diffusivity profiles indicated the possibility of a two-layered biofilm structure.

6. pH variations across the biofilms were insignificant.

Acknowledgments

The research was supported by the U.S. Department of Energy, Biological and Environmental Research Natural and Accelerated Bioremediation Program (NABIR) and the cooperative agreement EED-8907039 between the National Science Foundation and Montana State University. The authors thank Dr. Judy D. Wall for donating *Desulfovibrio desulfuricans* (G20).

Literature Cited

APHA, *Standard Methods for the Examination of Water and Wastewater*, 19th ed., American Public Health Association, Washington, DC (1995).

Beech, I. B., C. C. Gaylarde, J. J. Smith, and G. G. Geesey, "Extracellular Polysaccharides from *Desulfovibrio Desulfuricans* and *Pseudomonas Fluorescens* in the Presence of Mild and Stainless Steel," *Appl. Microbiol. Biotechnol.*, **35**, 65 (1991).

Beyenal, H., and Z. Lewandowski, "Combined Effect of Substrate Concentration and Flow Velocity on Effective Diffusivity in Biofilms," *Water Res.*, **34**, 528 (2000).

Bidoglio, G., P.N., M. Gibson, O. Gorman, and K. J. Roberts, "X-Ray Absorption Spectroscopy Investigation of Surface Redox Transformations of Thallium and Chromium on Colloidal Mineral Oxides," *Geochem. Cosmochim. Acta*, **57**, 2389 (1993).

Castro, J. M., B. W. Wielinga, J. E. Gannon, and J. N. Moore, "Stimulation of Sulfate-Reducing Bacteria in Lake Water from a Former Open-Pit Mine Through Addition of Organic Wastes," *Water Environ. Res.*, **71**, 218 (1999).

Coleman, M. L., D. B. Hedrick, D. R. Lovleys, D. C. White, and P. Kenneth, "Reduction of Fe(III) in Sediments by Sulfate-Reducing Bacteria," *Nature*, **361**, 436 (1993).

Elliot, P., S. Ragusa, and D. Catcheside, "Growth of Sulfate-Reducing Bacteria Under Acidic Conditions in an Upflow Anaerobic Bioreactor as a Treatment System for Acid Mine Drainage," *Water Res.*, **32**, 3724 (1998).

Fan, L. S., R. L. Ramos, K. D. Wisecarver, and B. J. Zehner, "Diffusion of Phenol Through a Biofilm Grown on Activated Carbon Particles in a Draft-Tube Three-Phase Fluidized Bed Bioreactor," *Biotechnol. Bioeng.*, **35**, 279 (1990).

Gibbs, J. T., and P. L. Bishop, "A Method for Describing Biofilm Surface Roughness Using Geostatistical Techniques," *Water Sci. Technol.*, **32**, 91 (1995).

Jeroschewski, P., C. Steuckart, and M. Kühl, "An Amperometric Microsensor for the Determination of H_2S in Aquatic Environments," *Anal. Chem.*, **68**, 4351 (1996).

Kühl, M., and B. B. Jorgensen, "Microsensor Measurements of Sulfate Reduction and Sulfide Oxidation in Compact Microbial Communities of Aerobic Biofilms," *Appl. Environ. Microbiol.*, **58**, 1164 (1992).

Kühl, M., C. Steuckart, G. Eickert, and P. A. Jeroschewski, "H_2S Microsensor for Profiling Biofilms and Sediments: Application in an Acidic Lake Sediment," *Aquat. Microb. Ecol.*, **15**, 201 (1998).

Lee, W., Z. Lewandowski, W. G. Characklis, and P. H. Nielsen, "Microbial Corrosion of Mild Steel in a Biofilm System," *Biofouling and Biocorrosion*, G. G. Geesey, Z. Lewandowski, and H. C-. Flemming, eds., Lewis, Boca Raton, FL, p. 205 (1994).

Lewandowski, Z., D. Webb, M. Hamilton, and G. Harkin, "Quantifying Biofilm Structure," *Water Sci. Technol.*, **39**, 71 (1999).

Lloyd, J. R., H.-F. Nolting, V. A. Solé, K. Bosecker, and L. E. Macaskie, "Technetium Reduction and Precipitation by Sulfate-Reducing Bacteria," *Geomicrobiol. J.*, **15**, 45 (1998).

Lovley, D. R., and E. J. P. Phillips, "Reduction of Uranium by *Desulfovibrio desulfuricans*," *Appl. Environ. Microbiol.*, **58**, 850 (1992).

Lovley, D. R. and E. J. P. Phillips, "Reduction of Chromate by *Desulfovibrio vulgaris* (Hildenborough) and Its c_3 Cytochrome," *Appl. Environ. Microbiol.*, **60**, 726 (1994).

Murga, R., P. S. Stewart, and D. Daly, "Quantitative Analysis of Biofilm Thickness Variability," *Biotechnol. Bioeng.*, **45**, 503 (1995).

Mizushina, T., "The Electrochemical Method in Transport Phenomena," *Adv. Heat Transfer*, **7**, 87 (1971).

Okabe, S., T. Matsuda, H. Satoh, T. Itoh, and Y. Watanabe, "Sulfate Reduction and Sulfide Oxidation in Aerobic Mixed Population Biofilms," *Water Sci. Technol.*, **37**, 131 (1998).

Okabe, S., P. H. Nielsen, W. L. Jones, and W. G. Characklis, "Sulfide Product Inhibition of *Desulfovibrio desulfuricans* in Batch and Continuous Cultures," *Water Res.*, **29**(2), 571 (1995).

Okabe, S., H. Satoh, T. Itoh, and Y. Watanabe, "Microbial Ecology of Sulfate-Reducing Bacteria in Wastewater Biofilms Analyzed by Microelectrodes and FISH (Fluorescent *In Situ* Hybridization) Technique," *Water Sci. Technol.*, **39**, 41 (1999).

Peyton, B. M., "Effects of Shear Stress and Substrate Loading Rate on *Pseudomonas Aeruginosa* Biofilm Thickness and Density," *Water Res.*, **30**, 29 (1996).

Picioreanu, C., M. C. M. van Loosdrecht, and J. J. Heijnen, "A Theoretical Study on the Effect of Surface Roughness on Mass Transport and Transformation in Biofilms," *Biotechnol. Bioeng.*, **68**, 536 (2000).

Postgate, J. R., *The Sulfate Reducing Bacteria*, 2nd ed., Cambridge Univ. Press, Cambridge (1984).

Power, M. E., J. C. Araujo, J. R. van der Meer, H. Harms, and O. Wanner, "Monitoring Sulfate-Reducing Bacteria in Heterotrophic Biofilms," *Water Sci. Technol.*, **39**, 49 (1999).

Santegoeds, C. M., T. G. Ferdelman, G. Muyzer, and D. de Beer, "Structural and Functional Dynamics of Sulfate-Reducing Populations in Bacterial Biofilms," *Appl. Environ. Microbiol.*, 3731 (1998).

Selman, J. R., and C. W. Tobias, "Mass Transfer Measurements by the Limiting Current Technique," *Advances in Chemical Engineering*, B. Drew, G. R. Cokelet, J. W. Hoopes, Jr., and T. Vermeulen, eds., Academic Press, New York, p. 211 (1978).

Shokes, T. E., and G. Möller, "Removal of Dissolved Heavy Metals from Acid Rock Drainage Using Iron Metal," *Environ. Sci. Technol.*, **33**, 282 (1999).

Smets, B. F., G. Riefler, U. Lendenmann, and J. C. Spain, "Kinetic Analysis of Simultaneous 2,4-Dinitrotoluene (DNT) and 2,6-DNT Biodegradation in an Aerobic Fluidized-Bed Biofilm," *Biotechnol. Bioeng.*, **63**, 642 (1999).

Stoodley, P., S. Yang, H. Lappin-Scott, and Z. Lewandowski, "Relationship Between Mass Transfer Coefficient and Liquid Flow Velocity in Heterogeneous Biofilms Using Microelectrodes and Confocal Microscopy," *Biotechnol. Bioeng.*, **56**, 681 (1997).

Tanyolaç, A., and H. Beyenal, "Prediction of Average Biofilm Density and Performance of a Spherical Particle under Substrate Inhibition," *Biotechnol. Bioeng.*, **56**, 319 (1997).

Thomas, R. C., *Ion-Sensitive Intracellular Microelectrodes: How to Make and Use Them*, Academic Press, London (1978).

Wall, J. D., B. J. Rapp-Giles, and M. Roussel, "Characterization of a Small Plasmid from *Desulfovibrio desulfuricans* and Its Use for Shuttle Vector Construction," *J. Bacteriol.*, **175**, 4121 (1993).

Xia, F., H. Beyenal, and Z. Lewandowski, "An Electrochemical Technique to Measure Local Flow Velocity in Biofilms," *Water. Sci. Technol.*, **32**, 3631 (1998).

Yang, S., and Z. Lewandowski, "Measurement of Local Mass-Transfer Coefficient in Biofilms," *Biotechnol. Bioeng.*, **48**, 737 (1995).

Yang, X., H. Beyenal, G. Harkin, and Z. Lewandowski, "Quantifying Biofilm Structure Using Image Analysis," *J. Microbiol. Methods*, **39**, 109 (2000).

Manuscript received July 31, 2000, and revision received Mar. 12, 2001.